NASA's Jet Propulsion Laboratory
Pasadena, California 91109-8099

Technical Support Package

Current Pulses Momentarily Enhance Thermoelectric Cooling

NASA Tech Briefs
NPO-30553

National Aeronautics and
Space Administration

Technical Support Package

for

CURRENT PULSES MOMENTARILY ENHANCE THERMOELECTRIC COOLING

NPO-30553

NASA Tech Briefs

The information in this Technical Support Package comprises the documentation referenced in **NPO-30553** of *NASA Tech Briefs*. It is provided under the Commercial Technology Program of the National Aeronautics and Space Administration to make available the results of aerospace-related developments considered having wider technological, scientific, or commercial applications. Further assistance is available from sources listed in *NASA Tech Briefs* on the page entitled "NASA Commercial Technology Team."

Additional information regarding research and technology in this general area may be found in a variety of publications available from the NASA Scientific and Technical Information (STI) Program Office. You can access the STI Program Office via **http://www.sti.nasa.gov** or as follows:

NASA STI Help Desk
NASA Center for AeroSpace Information
7121 Standard Drive
Hanover, MD 21076-1320

Telephone: (301) 621-0390, Fax: (301) 621-0134, E-mail: help@sti.nasa.gov

---

SUPERCOOLING OF PELTIER COOLER USING A CURRENT PULSE

G. Jeffrey Snyder[1], Jean-Pierre Fleurial[1], Ronggui Yang[2], Thierry Caillat[1], and Gang Chen[2].

jsnyder@jpl.nasa.gov
[1]Jet Propulsion Laboratory/California Institute of Technology
4800 Oak Grove Drive, Pasadena, CA 91109

[2]Mechanical Engineering Department,
Massachusetts Institute of Technology,
Cambridge, MA 02139

Abstract. The operation of a Peltier cooler can be temporarily enhanced by utilizing the transient response of a current pulse. The performance of such a device, using $(Bi,Sb)_2Te_3$ –based thermoelectric elements, was examined from –70°C to 55°C. We establish both theoretically and experimentally the essential parameters that describe the pulse cooling effect, such as minimum temperature achieved, maximum temperature overshoot, time to reach minimum temperature, time while cooled, and time between pulses. Using simple theoretical and semi-empirical relationships the dependence of these parameters on current pulse amplitude, temperature, thermoelectric element length, thermoelectric figure of merit and thermal diffusivity is established. At large pulse amplitudes the amount of pulse supercooling is proportional to the maximum steady state temperature difference. This proportionality factor is about half that expected theoretically. This suggests that the thermoelectric figure of merit, is the key materials parameter for pulse cooling. For this cooler, the practical optimum pulse amplitude was found to be about 3 times the optimum steady state current. A pulse cooler was integrated into a small commercial thermoelectric 3-stage cooler and provided several degrees of additional cooling for a period long enough to operate a laser sensor. The improvement due to pulse cooling is about the equivalent of two additional stages in a multi-stage thermoelectric cooler.

INTRODUCTION

A Peltier cooler uses the thermoelectric effect to transport heat with the application of an electric current. Under steady state conditions, the physics and engineering of such cooling devices is well studied [1] and in commercial use. The cooling coefficient of performance and maximum temperature drop depends on the properties of the thermoelectric materials used through the figure of merit, Z = $\frac{\alpha^2}{\rho\kappa}$, where α is the Seebeck coefficient, ρ is the electrical resistivity, and κ is the thermal conductivity. Briefly, this is because the heat removed due to the Peltier cooling, $Q = \alpha TI$, which is proportional to the applied current I, is counteracted by the Joule heating proportional to $I^2\rho$ and the reverse conductive heat flow proportional to κ. Since the Joule heat is proportional to a higher power of I than the Peltier cooling term, there will be a current, I_{max} which produces the largest temperature difference ΔT_{max}.

Peltier cooling occurs at the junction at the cold end of the thermoelectric elements. Joule heating, however occurs uniformly throughout the thermoelectric elements. Thus when current is applied, the cooling at the cold junction occurs before the Joule heat reaches the cold end. In this way, an applied current pulse $I > I_{max}$ can be used to temporarily produce a temperature difference greater than ΔT_{max}. This transient behavior of a thermoelectric cooler has been studied theoretically [2-7] with some experimental confirmation [6-10]. Such a cooler could be useful for a device such as a Mid-IR laser gas sensor, or other semiconductor device [11] that needs to be cold for a few milliseconds.

In this work, we attempt a thorough experimental investigation of a practical pulsed Peltier cooler to determine the minimum set of essential parameters and their relationships. A physical basis is used, when available, to explain these relationships. Such relationships can then be used to design a pulsed cooler.

In order to define terms, a summary of the theoretical problem and results are given. The theoretical analysis of the pulse cooling problem can be approximated into a one dimensional problem by assuming the n-type and p-type thermoelectric elements have exactly the same properties except for the opposite sign of the Seebeck coefficient. The differential equation is

$$\frac{\partial^2 T}{\partial x^2} + \frac{I^2\rho}{A^2\kappa} = \frac{\partial T}{a\partial t} \tag{1}$$

Here a is the thermal diffusivity, and A is the cross-sectional area. There are two boundary conditions. At x = 0 there is only Peltier cooling

$$\left.\frac{\partial T}{\partial x}\right|_{x=0} = \frac{\alpha I T(x=0)}{A\kappa} \tag{2}$$

and at $x = l$, where l is the length of the pulse thermoelectric elements, we have a hot side heat sink, $T(x=l,t) = T_h$.

The solution to the steady state problem for a meterials with Z independent of temperature [1] gives expressions for the current for maximum cooling $I_{max} = \alpha T_c A/\rho l$, the maximum steady state temperature difference $\Delta T_{max} = T_h - T_c = ZT_c^2/2$, and the cooresponding temperature profile $T_{SS}(x) = T_c + \Delta T_{max}(2x/l - x^2/l^2)$.

EXPERIMENTAL

Hot pressed n-$Bi_2Te_{2.85}Se_{0.15}$ and p-$Bi_{0.4}Sb_{1.6}Te_3$ were used to fabricate 5.8 mm tall thermoelectric elements with 1 mm^2 cross sectional area. The cold ends were Bi-Sn soldered to a 35 µm thick copper foil to which was soldered a 1 mil (25 µm) diameter Chromel-Constantin thermocouple for temperature measurement. The hot end was in the first case soldered an electrically isolated heat sink where the heat sink temperature could be adjusted from 55°C to –30°C. In the second case, the cooler was soldered to a commercial Marlow MI3021T-01AC 3-stage cooler with the top stage removed such that the cooling stages were connected in series as is done in a commercial cooler (Figure 1).

I_{max}, the steady state current that achieves the largest temperature difference was determined experimentally from a plot (at each hot side temperature) of cold side temperature vs. current, where the temperature was allowed to stabilize for 10 minutes for each point. For the single stage pulse cooler I_{max} = 0.675 A. The single stage pulse cooler was used for all measurements with a hot side temperature greater than –30°C. The three stage pulse cooler had a somewhat larger I_{max} = 0.75 A due to the larger I_{max} = 1.20 A of the Marlow Cooler.

The current was supplied and measured by a Keithley 2430 SourceMeter, which also measured the thermocouple temperature. The temperature data were recorded at speeds up to 3 Hz.

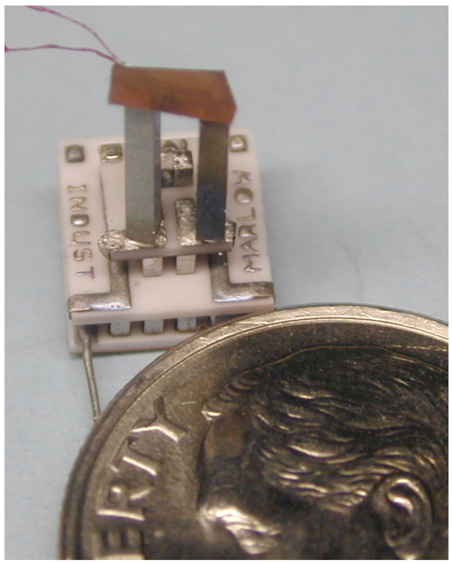

Figure 1. Three stage pulse cooler made from a commercial three stage cooler with top stage removed.

A square current pulse is used to achieve the supercooling as demonstrated in Figure 2. The temperature of the cold junction vs. time curve that is produced has the following general features. Starting from the maximum steady state cooling ($T = T_{ss}$, $I = I_{max}$) a current pulse ($P = I_{pulse}/I_{max}$) is applied at time = 0 which supercools the Peltier junction. The minimum temperature is achieved at some time t_{min}. This maximum difference between the supercooling temperature and the steady state temperature T_{ss}, which occurs at t_{min}, is ΔT_{pulse}. When the temperature returns to T_{ss} at time t_{ret}, the current is reduced to I_{max}. The temperature then rises rapidly to $\Delta T_{post\ pulse}$ above T_{ss}. Finally, the temperature will eventually return to T_{ss}, ready for the next pulse.

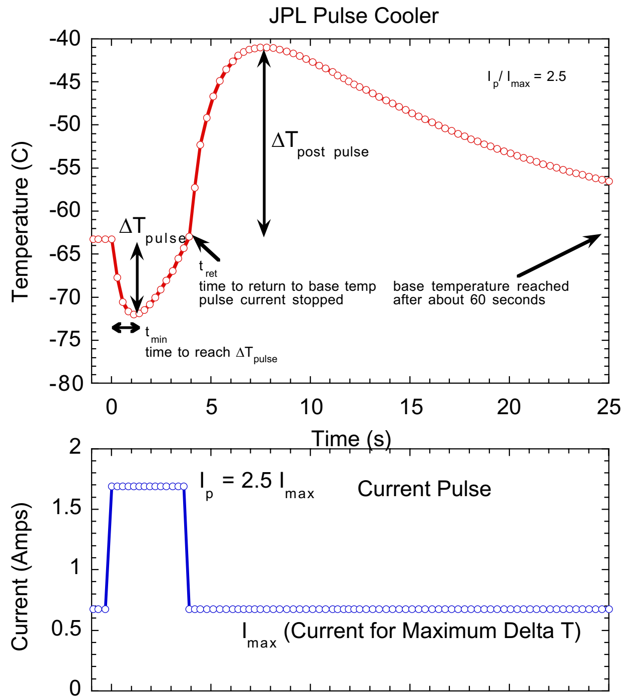

Figure 2 Example of Pulse cooling data with definitions of key variables

A series of experiments were conducted in which these parameters were taken from the Temperature vs. time curve for various pulse amplitudes and hot side temperatures. The fitting functions described below fit consistently well with single stage data for all measurements. The triple stage cooler shows the same trends but the curve fitting is not as good and therefore not used in many figures.

RESULTS

The characteristic times and temperatures defined in Figure 2, can be used to characterize the pulse cooler as a function of the independent variables such as, hot side temperature T_{hot}, length of pulse thermoelectric elements l, pulse factor P, and Z. This is useful not only to test theoretical models, but is very helpful when designing such a cooler where a user would want to easily calculate: the amount of increased cooling, the time the cooling lasts, the current needed and the time between pulses.

The magnitude of the current pulse P affects the lowest temperature achieved characterized by ΔT_{pulse} and is typically the focus of studies on pulse cooling. The analytical approximation of Babin [2] assumes the thermoelectric elements can be considered infinitely long. This approach is most appropriate for large pulses ($P > 2$) where the times involved are shorter than the characteristic thermal diffusion time constant. The transcendental solution, using the measured steady state properties, is shown in Figure 3 and predicts supercooling at infinite pulse $\Delta T_{P\infty} \approx \Delta T_{max}/2$.

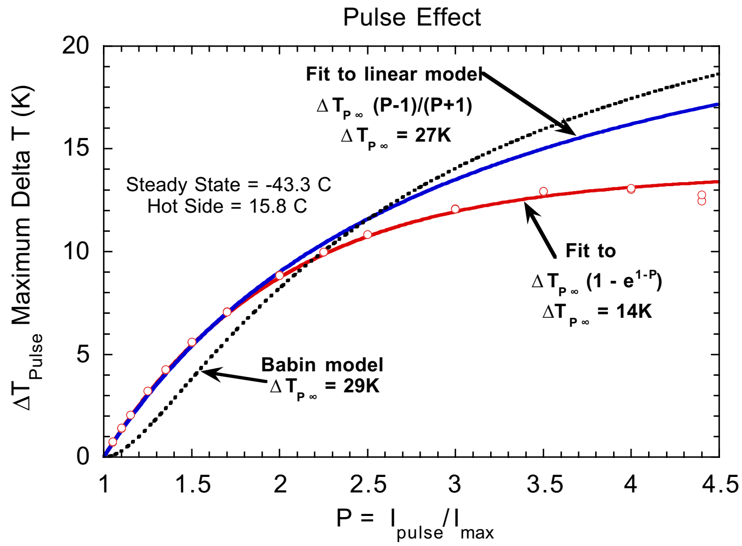

Figure 3. Maximum pulse cooling temperature difference as a function of pulse current.

A linear approximation [5] to the heat equation (equation 1) is perhaps more useful in explaining the experimental results:

$$\frac{\partial^2 T}{\partial x^2} + \frac{I^2 \rho}{A^2 \kappa} \approx \frac{T - T_{ss}}{at} \tag{3}$$

where the $x = 0$ boundary condition is also approximated to $\left.\frac{\partial T}{\partial x}\right|_{x=0} \approx \frac{\alpha I T_c}{A\kappa}$. The general solution is

$$\frac{T(x,t) - T_{ss}}{zT_c^2} = (P^2 - 1)\tfrac{at}{l^2} - (P-1)\tfrac{\sqrt{at}}{l} e^{-x/\sqrt{at}} \tag{4}$$

which predicts an algebraic function for ΔT_{pulse}

$$\Delta T_{pulse} = \Delta T_{P\infty}\left(\frac{P-1}{P+1}\right) \tag{5}$$

with $\Delta T_{P\infty} = \Delta T_{max}/2$. This function fits well (Figure 3) to the experimental data for small pulses with a $\Delta T_{P\infty}$ slightly smaller than that expected. Both theoretical forms give the correct order of magnitude but both deviate significantly from the experimental shape, particularly at large pulse amplitudes where both models predict a further increase in ΔT_{Pulse} above $P = 3$ which is not observed experimentally. The experimental data fit well to the empirically determined formula $\Delta T_{Pulse} = \Delta T_{P\infty}$ $(1 - e^{1-P})$ with only one free parameter. The data at the highest pulse amplitudes ($P > 3$) have higher standard deviations and deviate from the exponential trend. This may due to the experimental uncertainty when measuring these fast pulses, or simply due to the thermal diffusion time from the junctions to the thermocouple.

The excellent fit to the empirical exponential form allows us to characterize ΔT_{Pulse} for all P with one parameter $\Delta T_{P\infty}$. It has already been suggested from the above models that $\Delta T_{P\infty}$ is related to ΔT_{max}. This is confirmed experimentally in Figure 4. Here $\Delta T_{P\infty}$ mimics ΔT_{max}, decreasing as the hot side temperature is lowered. As a consequence of the approximate relationship, $\Delta T_{P\infty} \approx \Delta T_{max}/4 = ZT_c^2/8$, it appears the only materials parameter that effects the minimum temperature achieved is the thermoelectric figure of merit Z.

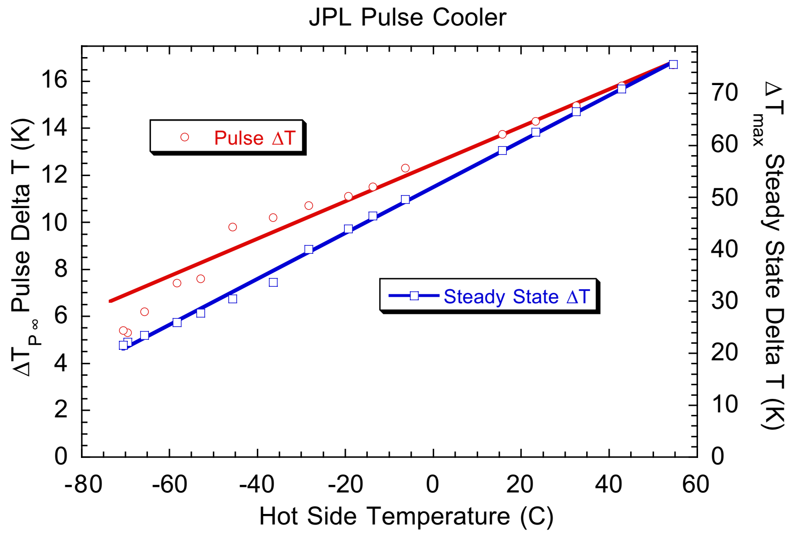

Figure 4. Maximum pulse cooling compared to maximum steady state cooling.

As the pulse amplitude increases, the minimum junction temperature is lower, but for a shorter time. Figure 5 shows the decrease in t_{min} and t_{ret} as P increases for a single hot side temperature. The data for t_{min} fit very well to a $(P + 1)^{-2}$ dependence. This can be explained by the linear approximation (eq. 3, 4) which predicts

$$t_{\min} = \frac{t_{ret}}{4} = \frac{l^2}{4a(P+1)^2} = \frac{\tau}{(P+1)^2} \tag{6}$$

where $\tau = \frac{l^2}{4a}$

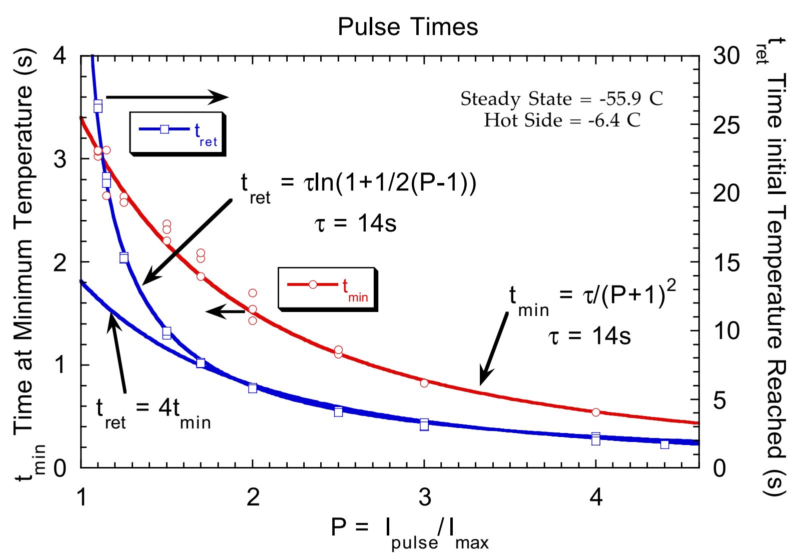

Figure 5. Pulse dependence of characteristic times t_{min} and t_{ret}.

The data for t_{ret} are well described by the linear model when P is large or t_{ret} is short. The crossover occurs at about time $t = \tau = 14$ s. For times greater than τ, a quasi-steady state model described below can explain the experimental data. The corresponding curves from Babin's model [2] are unphysical for $P < 3$ and therefore not included in Figure 5.

The two characteristic times t_{min} and t_{ret} can be used to estimate the time below a specified temperature in the supercooled state, providing the shape of the temperature pulse is roughly constant. If using the reduced variables $(T - T_{ss})/\Delta T_{Pulse}$ and t/t_{ret}, the result of the linear model predicts a constant shape of temperature pulse

$$\frac{T - T_{SS}}{\Delta T_{pulse}} = 4\left(\frac{t}{t_{ret}} - \sqrt{\frac{t}{t_{ret}}}\right) \tag{7}$$

The pulse shapes predicted by the analytical model of Babin [2] are very similar to that of the linear model, becoming nearly identical for small P. The experimental data of Figure 6 clearly show the transition between two regimes. For large P which take short times, the curves are similar in shape to that predicted by the linear model. For $t < t_{min}$ the cooling is progressively slower than eq. 7 as P increases, which may be due to the time for the cooling to reach the thermocouple. It is expected that in an actual application $P > 2$ will be used, in which case the pulse cooling shape is nearly constant and given, to a reasonable approximation, by eq. 7. For longer times (smaller P) greater than the thermal diffusion time (14s) there is an exponential decay component in the measured curves. This provides a strong deviation in the pulse shape most noticeable in the P = 1.05 curve.

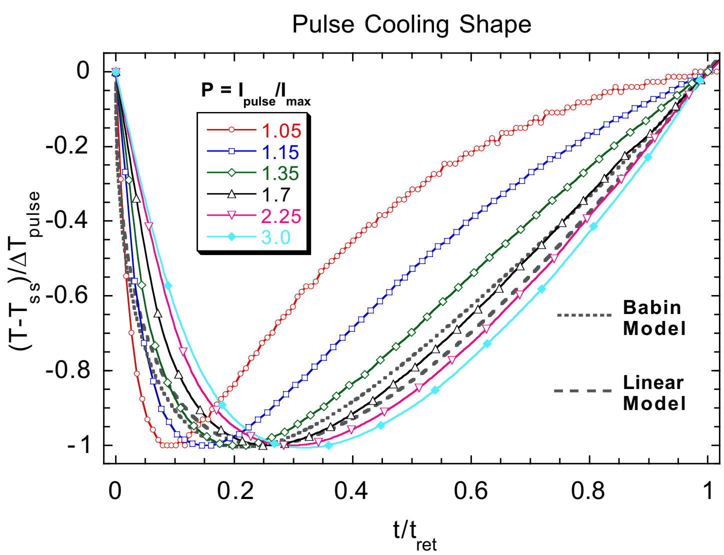

Figure 6. Shape of pulse cooling curve using reduced variables.

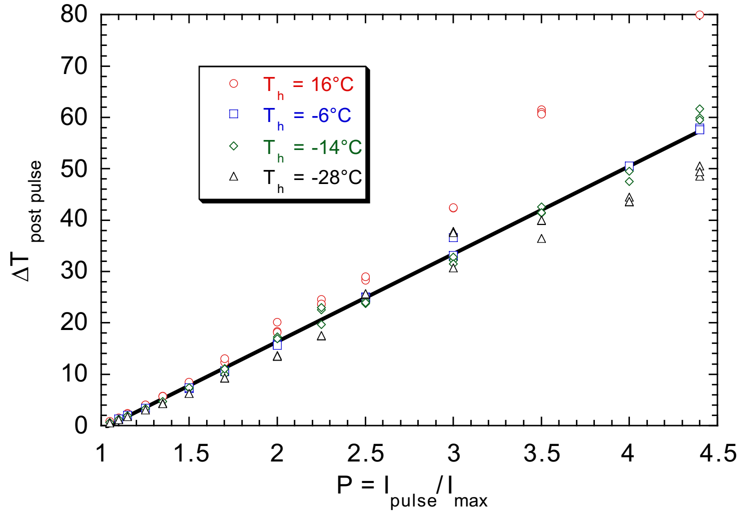

Figure 7. Junction heating $\Delta T_{Post\ Pulse}$ after supercooling pulse. Line is fit to –6°C data

After the supercooling, the junction rapidly heats up reaching $\Delta T_{Post\ Pulse}$ above T_{ss}. For temperature sensitive electronics, this may be a factor in cooler design. Figure 7 shows the maximum temperature rise after pulse operation, defined as $\Delta T_{Post\ Pulse}$ in Figure 2. The magnitude of $\Delta T_{Post\ Pulse}$ will depend on the amount of excess Joule heating added to the system during pulse operation. One might expect then that $\Delta T_{Post\ Pulse}$ will be proportional to the excess heating rate (P^2 –1) and a heating time, an obvious choice being t_{ret}. Much of the $\Delta T_{Post\ Pulse}$ data is extremely linear, proportional to (P –1) as seen in Figure 7, which is off by a factor of (P + 1) if using the t_{ret} of eq. 6. Obviously, if the pulse lasts longer (shorter) than t_{ret}, $\Delta T_{Post\ Pulse}$ will be larger (smaller). In practice, the optimum pulse time will be between t_{min} and t_{ret}.

The time required to return to the steady state condition can be characterized by an exponential decay time constant, which is derived as follows. If we define $\Delta T = T - T_{ss}$ then for $I = I_{max}$, the heat equation (eq. 1) reduces to

$$\frac{\partial^2 \Delta T}{\partial x^2} = \frac{\partial \Delta T}{a \partial t} \tag{8}$$

Thus, after the application of pulse current, the perturbation in temperature will return to the steady state temperature profile according to eq. (8). The series solution [12] to this equation has as the fundamental exponential decay Exp[$\pi^2 at/4l^2$] with time constant $\tau = 4l^2/\pi^2 a$. The higher order terms have shorter time constants and smaller amplitudes. The data at long times fit well to this form (Figure 8). For the single stage cooler the measured time constant for all hot side temperatures is 13.7 s ± 0.6 s which implies a thermal diffusivity of 0.010 cm^2/s. Independent measurements of thermal diffusivity for these Bi_2Te_3 materials gives 0.007 cm^2/s at room temperature..

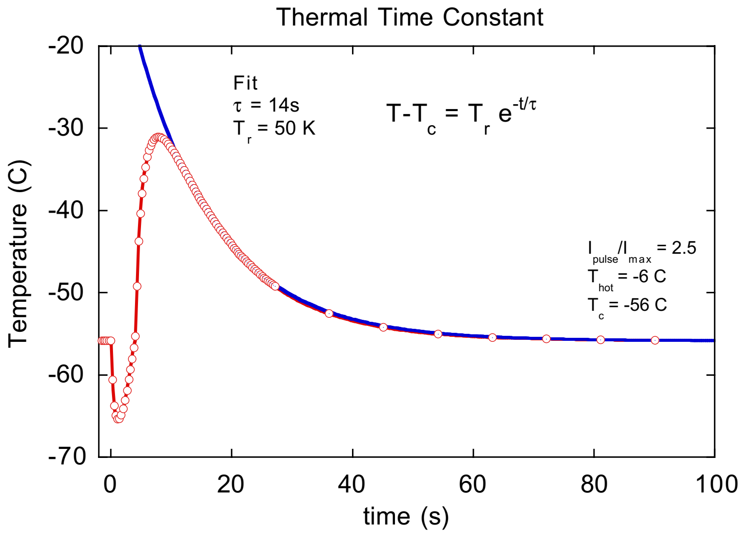

Figure 8. Post pulse thermal decay to steady state.

We can apply this thermal decay result to develop a quasi steady state model to explain the $t > \tau$ regime. If we assume that a change in current will produce a evolution from the initial state to the final state with the primary functional form being Exp[$-\pi^2 at/4l^2$], then we can derive a simple equation for t_{ret}. This should be particularly valid for times greater than the thermal time constant of the thermoelectric element (14s in this case). The initial state relative to T_{ss}, $-\Delta T_i$, should be proportional to the supercooled junction temperature approximated by eq. (5), or by fitting to experimental data. In either case, for $P \approx 1$ this reduces to $\Delta T_i \approx C(P - 1)\Delta T_{Max}/4$, where C is the proportionality constant. The final state junction temperature is the steady state value for that current which can be found experimentally from steady state temperature *vs.* current curves which can be fit to $\Delta T_f \approx C_2\Delta T_{Max}(P - 1)^2$ where C_2 is a fitting constant approximately equal to 1. t_{ret} is then the time is takes the exponential $\Delta T_f - (\Delta T_f + \Delta T_f)$Exp[$-t/\tau$] to decay to zero, giving $t_{ret} = \tau ln(1 + C/4(P - 1))$. The fit to this equation (Figure 5) is remarkably good for $C = 2$, even for large P. This suggests that this analysis is valid for larger P with $\Delta T_i = C\Delta T_{Pulse}$ (from eq. 5) where $C = (P + 1)$

DISCUSSION

Initial experiments of thermoelectric pulse coolers have varying results. Early measurements that use the thermoelectric elements themselves as temperature probes [7-9] indicate more supercooling than we observed. Results where a separate thermocouple [6, 10] is used for temperature measurement are consistent with our results, with less detail.

Despite the many dependent and independent variables, the characteristic temperatures and times of a pulse cooler can be well modeled with a few simple empirical relationships. In many cases these relationships have a theoretical basis. Such models can be simply used to judge the appropriateness of a pulse cooler for a specified application.

The two theoretical models discussed above predict a maximum pulse cooling $\Delta T_{P\infty} = \Delta T_{max}/2$, about twice that observed here. Both models neglect the interconnect and any time required for the junction cooling to reach the thermocouple. To test the effect of the interconnect, a similar device was fabricated with no copper interconnect by soldering n- and p-type thermoelectric elements directly together with a thermocouple in the solder junction. This configuration was also used in [6-8]. The results were essentially the same (also found in [6]), with ΔT_{Pulse} 90% of that observed in Figure 3.

Two regimes are clearly distinguishable in the experimental data. For times shorter than the thermal relaxation time the data follows simple transient models. For longer times thermal decay exponential forms are more appropriate. Numerical simulations can be used to model both regimes and can qualitatively reproduce the reported data [13].

The series connection of the pulse cooler with other stages to form a multi stage pulse cooler worked well. The performance was consistent with the results obtained for the single stage pulse cooler despite that fact that the cooling ability of the small cooler is much less than the heat sink used for the single stage pulse cooler. For optimum performance, the A/l ratio of the pulse cooling stage should be optimized so that the I_{max} is the same for all stages. The heat removal capacity of the pulse cooler is expected to be similar to that of a standard thermoelectric cooler with similar cross-sectional areas.

The original three stage cooler has ΔT_{max} = 98.9 K (with an additional 1K from pulsing) from a hot side temperature of 17°C where I_{max} = 1.2 A. At the same hot side temperature, the pulse cooler ΔT_{max} = 92.9 K was less, primarily due to the mismatch in I_{max} mentioned above. At optimal pulse a cooling difference of $\Delta T_{max} + \Delta T_{Pulse}$ = 102.0 K was observed. For a pulsed cooler with matched I_{max} a temperature difference of 108K would be expected. This is a 9% improvement compared to the unpulsed cooler, and about the equivalent of a 5 stage cooler.

CONCLUSIONS

The characteristics of a thermoelectric pulse cooler has been analyzed by determining and modeling the characteristic times and temperatures during the pulsing cycle for various pulse amplitudes and steady state temperatures. The amount of super cooling ΔT_{Pulse} has been found to be a simple function of pulse amplitude steady state temperature. At large pulse amplitudes the amount of pulse supercooling is about 1/4 of the steady state cooling, for a wide range of temperatures. This suggests that the thermoelectric figure of merit, Z, is the key materials parameter for pulse cooling. The practical optimum pulse amplitude is found to be about 3 times the optimum steady state current.

The time to reach minimum temperature and the time below a specific temperature can be predicted with a simple equation, derived from simplifications to the heat equation. Both times decrease as the current pulse is increased. After pulse cooling, the sample will overheat by an amount that can be predicted by a simple empirical relationship. The return to steady state temperature follows a simple exponential decay. All the characteristic times are proportional to the square of the thermoelectric element length, providing a simple framework to optimize a pulse cooler's geometry for a specific application.

A pulse cooler was integrated into a small commercial thermoelectric 3-stage cooler and provided several degrees of additional cooling for a period long enough to operate a laser sensor. The improvement due to pulse cooling is about the equivalent of two additional stages in a multi-stage cooler.

ACKNOWLEDGMENTS

This work was carried out by the Jet Propulsion Laboratory, California Institute of Technology, under contract with the National Aeronautics and Space Administration. Funding support came from DARPA HERETIC program. We would like to thank Hylan Lyon at Marlow Industries for providing the MI3021T-01AC cooler. Comparisons with numerical simulations were done by Ronggui Yang, A. Ravi Kumar and Gang Chen at UCLA/MIT. GJS would also like to thank Satwindar Sadhal at USC for discussions on thermal transport theory.

REFERENCES

[1] R. R. Heikes and R. W. Ure, *Thermoelectricity: Science and Engineering* (Interscience, New York, 1961).
[2] V. P. Babin and E. K. Iordanishvilli, *Soviet Physics - Technical Physics* **14**, 293 (1969).
[3] J. E. Parrott, *Solid State Electronics* **1**, 135 (1960).
[4] G. E. Hoyos, K. R. Rao, and D. Jerger, *Energy Conversion* **17**, 23 (1977).
[5] A. Miner, A. Majumdar, and U. Ghoshal, *Applied Physics Letters* **75**, 1176 (1999).
[6] L. S. Stil'bans and N. A. Fedorovich, *Soviet Phys. Tech. Phys.* **3**, 460 (1958).
[7] K. Landecker and A. W. Findlay, *Solid-State Electronics* **3**, 239 (1961).
[8] M. Idnurm and K. Landecker, *Journal of Applied Physics* **34**, 1806 (1963).
[9] G. E. Hoyos, K. R. Rao, and D. Jerger, *Energy Conversion* **17**, 45 (1977).
[10] R. L. Field and H. A. Blum, *Energy Conversion* **19**, 159 (1979).
[11] T. Yamamoto, *Proceedings of the IEEE* **56**, 230 (1968).
[12] E. C. Zachmanoglou and D. W. Thoe, *Introduction to Partial Differential Equatinos with Applications* (Dover Publications, New York, 1986) p340.
[13] R. Yang, G. Chen, and et.al, in *MRS*, (2001).